STRATIGRAPHICAL SEQUENCES OF SCHRÖDINGER BASIN ON THE MOON. Y. Meng[1], M. Ding[1], M.-H. Zhu[1], and L. Y. Xu[1], [1]State Key Laboratory of Lunar and Planetary Sciences, Macau University of Science and Technology, Macau, China (mhzhu@must.edu.mo).

Introduction: The Schrödinger basin, centered at 75.0° S and 132.5° E on the far side of the Moon, has a diameter of ~320 km and an average depth of 4.5 km. It is the best-preserved peak-ring basin on the Moon due to its young formation age of lower Imbrian epoch (~3.85-3.8 Ga) [1-4]. Schrödinger is located within the South Pole–Aitken basin, the oldest, largest, and most geologically complex basin on the Moon. The unique location and formation time of the Schrödinger basin makes it of particular scientific interest to study complex geologic processes before and after the Schrödinger impact, in addition to the impact event itself [1,3]. As a fascinating landing site with huge potential, Schrödinger is targeted by many lunar exploration missions, such as Draper's SERIES-2 lander and ESA's Heracles spacecraft, for studying various key planetary processes from lunar differentiation to volcanic eruption [5].

Previous studies have classified the basin into various geological units [1-3, 6]. *Kramer et al.* [3] use Moon Mineralogy Mapper (M^3) spectral data, combined with optical images and topography data, to provide the most detailed division of geologic units. Within the basin floor, the peak ring (unit pNpr in Fig. 1a) forms first by the uplift of pre-impact crustal materials, followed by the collapsed basin wall materials (Iw) composed of impact ejecta. The most extensive geologic units in this region are shock-melt materials from Iipr to Isip with increasing melt contents.

After the formation of the basin, two dark volcanic units, Em and Ep, deposited in the basin floor. One of the units, Ep, is southwest of a long graben (segment F1 in Fig. 1a), which makes *Kramer et al*. [3] suggest that the formation of this graben may be caused by volcanic activities. However, *Shoemaker et al*. [2] noticed the striking concentric and radial patterns of the graben system and attributed its origin to the isostatic rebound after the basin formation. The origin of the graben system can only be determined after estimating its relative age to the plain units and volcanic deposits.

The model age of each geologic unit can be determined by counting small craters superposing on. The Schrödinger basin has previously been dated by *Mest et al.* [6], who counted craters with diameters larger than 1 km for each unit based on Clementine UVVIS images (>100 m/pixel) and determined the relative ages of the geologic units. The plain materials are estimated to form in the Imbrian period. For the volcanic materials, Ep is estimated to form in Eratosthenian whereas Em in the upper Imbrian epoch. But two alternative studies [2,3] estimated Ep to be Eratosthenian. The age of Ep is thus under debate.

In this study, we use Kaguya Terrain Camera (TC) images with a higher resolution of 10 m/pixel to estimate the model ages for six geologic units and multiple graben segments. The high-resolution images allow the identification of smaller sized craters down to 100 m in diameter, which could help determine the formation ages of the geological units more accurately, and thus clarify the stratigraphical sequence within the Schrödinger basin and understand the origin of the graben system.

Data and Methods: For the absolute model age (AMA) estimation, we use Kaguya TC images [7] in combination with the regional geologic map [3]. For each of the six major geologic units, we select one to four smooth sub-regions (boxes A-J in Fig. 1a) with intermediate illumination angles and no obvious secondary craters. We do not date the peak ring and basin wall units due to the steep slope in those regions. We then perform traditional cumulative size-frequency distribution (CSFD) measurements [8, 9] and obtain the AMAs based on the crater production function of [9].

To determine the model ages for the grabens, we employ the buffered crater counting (BCC) methodology [7, 8]. For the linear graben segments with limited craters, this technique effectively extends the dating area by incorporating more craters formed later than the studied region, thus boosting statistical reliability of crater counting results [9].

Results and Discussion: For the plain units, we estimate the model ages to be 3.78-3.71 Ga for Irh, 3.77-3.64 Ga for Ish, 3.70-3.52 Ga for Isop, and 3.65-3.49 Ga for Isip, consistent with previous age estimates of the Imbrian period [6]. These dated regions are all shock-melt materials but with varied melt contents. Our dating results confirm the trend that regions with more melts are younger [3].

In addition to the plain region, we also date the volcanic regions. The estimated model ages for the entire units Ep and Em are 2.25-2.13 Ga and 2.42-2.36 Ga, respectively. For comparison, our estimated model age for the selected sub-region J within the unit Ep is 2.27-2.25 Ga, consistent with the estimated model age for the entire unit. The volcanic unit Ep is found to erupt after the formation of graben based on mineral content analyses [2, 3]. We confirm it by dating the volcanic filled area above the graben segment F1, yielding a model age of 2.31-2.18 Ga. This age is younger than our estimated

model age for the graben system (see the next paragraph) but lies in the estimated age range of the volcanic unit. Therefore, our dating results support the post-graben volcanic eruption scenario. Both volcanic regions within Schrödinger are dated to form in the Eratosthenian period, consistent with the results of [3]. But this age is much younger than the proposed formation age in the upper Imbrian period by [2] merely based on visually inspection of the Clementine UVVIS images with a considerably lower resolution. We thus propose the younger Eratosthenian age is more reliable. This is plausible because the lunar thermal activities are considered to be strong at the Eratosthenian [10].

For the graben segments, we estimate their model ages to be in a range of 3.78-3.41 Ga. This formation period is right after the formation of the Schrödinger basin but far before the post-impact volcanic deposits (Fig. 1b). The temporal overlap between the plain and graben formation suggest that the graben system forms during the period of post-impact isostatic adjustment of the basin [2]. In this period, the entire basin can be uplifted if the lithosphere is cold enough to mechanically act as an integrated plate in response to the buoyancy of the impact-induced thickened crustal annulus [11-13]. The uplift of the basin could then induce horizontal tensile stress and generate concentric and radial grabens [14]. But as this post-impact isostatic adjustment only last for tens of millions of years, the reason why the graben system lasted for such a long period deserves further investigation. We also notice a deviation from the regionally dominated concentric pattern in the southern graben segment F3. This is spatially correlated with a pre-existing thickened crust [15] due to the much older Amundsen-Ganswindt basin. The crustal thickness variations may influence the regional stress state and graben distribution.

There is a notable time gap of ~ 1 Gyr between the grabens and volcanic deposits. This extended time gap suggests that the volcanic activities cannot be directly controlled by the graben system. Instead, a compositional or thermal anomaly of the underlying mantle is likely more responsible for the volcanic activities, although a deep graben or fracture system is required to provide the eruption channel.

Conclusions: We estimate the formation times for the different geologic units from plains and volcanic deposits to grabens in the Schrödinger basin using conventional and buffered crater counting techniques, based on Kaguya TC images. We find both the plain units and grabens are developed in the Imbrian period; the close temporal overlap implies that the grabens may be induced by isostatic adjustment after the basin formation. But the volcanic units are estimated to form in the Eratosthenian period and long after the plain and graben formation, implying that the mantle source, instead of the regional stress state, controls the volcanic activities in the Schrödinger basin.

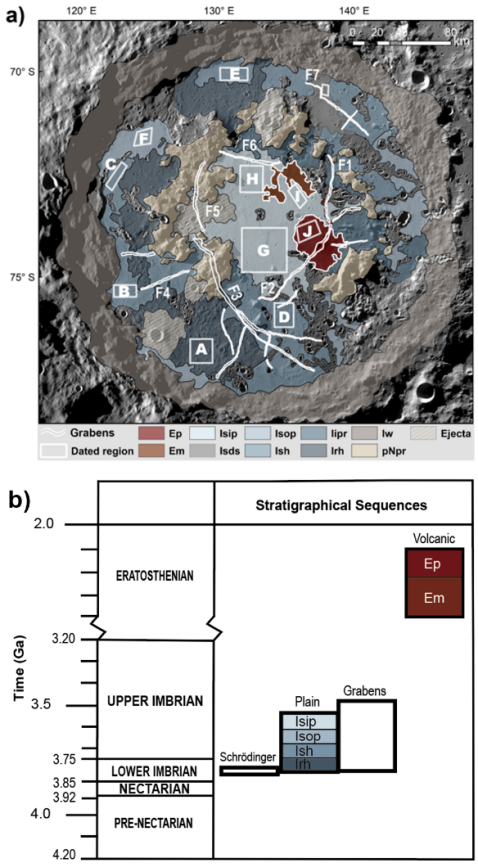

Figure 1. a) Major geologic map of the Schrödinger basin on a polar stereographic projection, modified after [3]. The base map is LRO WAC mosaic. Colored regions are different geologic units. White lines are Fractures F1-7. White boxes A-J indicate the regions we select for dating. b) Stratigraphical sequence of the Schrödinger basin based on our dating results.

Acknowledgements: This work is supported by the Science and Technology Development Fund, Macau (0020/2021/A1; 0064/2022/A2) and NSFC 12173106.

References: [1] Wilhelms et al. (1987) *USGS,* 1348. [2] Shoemaker et al. (1994) *Science,* 266, 1851. [3] Kramer et al. (2013) *Icarus,* 223, 131. [4] Kring et al. (2016) *Nat Comm*, 7, 1-10. [5] Morse et al. (2021) *PSJ,* 2, 167. [6] Mest et al. (2011) *GSA SP* 477, 95. [7] Haruyama et al. (2008) *EPP,* 60, 243–255. [8] Hiesinger et al. (2000) *JGR*, 105, 29239-29275. [9] Neukum er al. (2001) *SSR,* 96, 55 – 86. [10] Li et al. (2021) *Nature*, 600, 54-58. [11] Melosh et al. (2013) *Science*, 340, 1552–1555. [12] Freed et al. (2014) *JGR,* 119, 2378–2397. [13] Ding & Zhu. (2022) *JGR,* 127. [14] Kamata & Nimmo. (2014) *JGR,* 119, 2272–2289. [15] Wieczorek et al. (2013) *Science,* 339, 671–675.